Science of the Total Environment xxx (xxxx) xxx

Contents lists available at ScienceDirect

Science of the Total Environment

journal homepage: www.elsevier.com/locate/scitotenv

Groundwater contamination assessment in Ulaanbaatar City, Mongolia with combined use of hydrochemical, environmental isotopic, and statistical approaches

Bayartungalag Batsaikhan [a,b], Seong-Taek Yun [a,*], Kyoung-Ho Kim [a,c], Soonyoung Yu [d], Kyung-Jin Lee [a], Young-Joon Lee [c], Jadambaa Namjil [b]

[a] Department of Earth and Environmental Sciences, Korea University, Seoul 02841, Republic of Korea
[b] Institute of Geography and Geoecology, Mongolian Academy of Sciences, Ulaanbaatar 15170, Mongolia
[c] Korea Environment Institute, Sejong 30147, Republic of Korea
[d] Korea-CO_2 Storage Environmental Research (K-COSEM) Research Center, Korea University, Seoul 02841, Republic of Korea

HIGHLIGHTS

- Degradation of urban groundwater quality in Ulaanbaatar, Mongolia is significant.
- Nitrate contamination is land-use dependent and originates from sewage effluents.
- Hydrochemical and isotopic data are evaluated using a PCA bi-plot.
- Subcomposition of NO_3^-, Cl^-, and SiO_2 represents major hydrochemical processes.
- Groundwater quality index (GQI) is proposed to evaluate groundwater quality status.

GRAPHICAL ABSTRACT

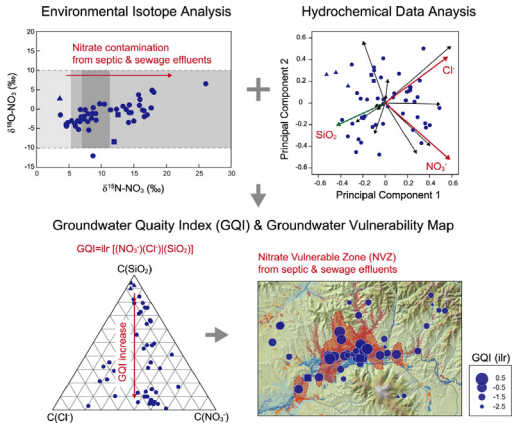

ARTICLE INFO

Article history:
Received 13 March 2020
Received in revised form 12 September 2020
Accepted 29 September 2020
Available online xxxx

Editor: Jurgen Mahlknecht

Keywords:
Urbanization
Peri-urban, Mongolia
Nitrate contamination
Sewage and pit latrine
Water chemistry and environmental isotope
Groundwater Quality Index (GQI)

ABSTRACT

Ulaanbaatar City, Mongolia is rapidly becoming urbanized and attracts great attention because of environmental issues. This study was performed to assess the status of groundwater quality in Ulaanbaatar at an early but growing stage of urbanization, focusing on nitrate contamination in relation to land use. Along with high total dissolved solids and NO_3^- concentrations, significant contamination of groundwater is indicated by positive loadings of NO_3^-, Cl^- and $\delta^{15}N\text{-}NO_3^-$ along the first principal component of the principal component analysis (PCA). Based on the concentrations and $\delta^{15}N$ values of nitrate, groundwater is classified into two groups: Group I (baseline quality) and II (contaminated). Nitrate in Group II water in urbanized (esp. peri-urban) areas is higher in concentration (> 10 mg/l NO_3^-) and N-isotopic values (> 10‰ $\delta^{15}N\text{-}NO_3^-$), while pristine hydrochemistry is observed restrictedly in grassland and forest areas. Other ions (e.g., Cl^- and SO_4^{2-}) are also higher in Group II water. The $\delta^{15}N\text{-}NO_3^-$ values in Group II water in combination with the spatial distribution on the land use map indicate that nitrate originates from untreated sewage effluents including pit-latrine leakage in peri-urban areas, while nitrate in Group I water originates from soil organic matter. The relationship between nitrate concentrations and δ^2H (and $\delta^{18}O$) values of water suggests that nitrate enrichment is also influenced by evaporation during groundwater recharge. With the help of PCA for compositional data, we suggest a hydrochemical index for groundwater contamination assessment; i.e., the Groundwater Quality Index (GQI)

* Corresponding author.
E-mail address: styun@korea.ac.kr (S.-T. Yun).

https://doi.org/10.1016/j.scitotenv.2020.142790

that consists of three variables (concentrations of dissolved silica, nitrate and chloride) and can be used to delineate zones vulnerable to nitrate contamination as a crucial step for the efficient monitoring and management of groundwater quality. The study results suggest an urgent need for the management of unsealed pit latrines that are common in peri-urban areas with high population density.

1. Introduction

Urbanization has accelerated around the world, and it is expected that about 2.5 billion people will be added to the urban population by 2050, with nearly 90% of the increase in Asia and Africa (United Nations, 2019). Urbanization is a particular concern in developing countries, where the water supply for drinking and sanitation purposes is insufficient to sustain the rapid population growth (Foster, 2001; Vairavamoorthy and Mansoor, 2006). Therefore, water scarcity is emerging as one of the most important challenges in rapidly urbanizing countries (Bao and Fang, 2007; Kong et al., 2019), together with climate change, which is projected to increase the frequency and severity of droughts globally (Semadeni-Davies et al., 2008). Moreover, such rapid population increases in urban areas result in significant water quality problems, which are caused by the discharge of urban wastewater mainly due to the improper management of sanitary sewage, drainage and waste disposal; practically, many cities with unsewered residential development have suffered from significant surface and ground water contamination (Foster, 2001; Barrett and Howard, 2002; Chambers et al., 2016; Shi et al., 2019).

For example, approximately 1.3 million people live in Ulaanbaatar, the capital of Mongolia (i.e., nearly 47% of the nation's total population in 2014; SDOU, 2015) and the population has grown rapidly during the last decade (by 3.5% per year) because of massive rural-to-urban migration (Bayanchimeg and Batbayar, 2013). Urbanization, coupled with climate conditions, has resulted in many environmental problems including the degradation of groundwater quantity and quality (Kamata et al., 2010; Batsaikhan et al., 2018; Dalai et al., 2019). In particular, each house plot (470–590 m^2) in peri-urban areas is surrounded by a wooden fence in which a detachable felt tent (55 to 77 m^2), pit latrine, and garbage bin are located without basic infrastructure such as communal heating and sewerage (Kamata et al., 2010; Byambadorj et al., 2011). The large number of pit latrines (about 75,000 units) (UN-HABITAT, 2010; Byambadorj and Lee, 2019) and poor sanitary facilities are considered to be a major source of groundwater nitrate pollution in the peri-urban area (Bock, 2014; Batsaikhan et al., 2018). However, the status of groundwater quality has rarely been studied here as in many other peri-urban areas in developing counties (Foster, 2001; Barrett and Howard, 2002).

Groundwater contamination is generally assessed based on hydrochemical and environmental isotopic (e.g., dual isotopic compositions of nitrate) data by means of multivariate statistical analysis (e.g., Clark and Fritz, 1997; Mengis et al., 1999; Fukada et al., 2003; Choi et al., 2010; Kendall and Aravena, 2000; Tsujimura et al., 2007a, 2007b; Hosono et al., 2011; Dogramaci et al., 2012; Jurado et al., 2013; Chambers et al., 2016; Lee et al., 2019). Principal component analysis (PCA) is one of the most popular multivariate statistical approaches to identify an underlying structure by reducing the dimensions of original variables to a few principal components (PCs). Recent studies have shown that PCA using log-ratio transformed data is more successful in exploring the relative changes of hydrochemical data in groundwater (e.g., Buccianti et al., 2014; Engle and Blondes, 2014; Engle and Rowan, 2014). In particular, the isometric log-ratio (ilr) transformation was found to yield more robust PCA results for compositional data with insignificant outliers (Egozcue et al., 2003; Egozcue and Pawlowsky-Glahn, 2005), while the PCA of centered log-ratio (clr) data is useful to visualize combinations of processes (Engle and Blondes, 2014). We noticed that the ilr transformation has an orthonormal basis and preserves angles between original compositional data (Egozcue et al., 2003; Filzmoser et al., 2010) when it converts the data to a Euclidean space. The ilr coordinates of subcomposition representing groundwater contamination may be suggested as an index to evaluate the status of groundwater quality because they have the form of a chemical composition ratio (see Section 2.3).

The main objectives of this study are (1) to assess the hydrochemistry of urban groundwater in the fast-growing Ulaanbaatar City, Mongolia in 2011; (2) to examine the sources of anthropogenic contamination (esp. nitrate contamination); (3) to identify major hydrochemical processes; and (4) to analyze subcomposition representing groundwater contamination. For these purposes, we have analyzed and interpreted hydrochemical data in conjunction with $\delta^{15}N$ and $\delta^{18}O$ of nitrate and $\delta^{18}O$ and $\delta^{2}H$ of water, and suggest one of the ilr coordinates of the subcomposition as the Groundwater Quality Index (GQI) for the overall evaluation of the degree of anthropogenic contamination as an important step for the management of groundwater quality. We also suggest proper controls for groundwater contamination. The assessment result of groundwater contamination at an early but growing stage of urbanization in a fast-growing city provides implications for groundwater management in many other rapidly urbanizing cities around the world with unsewered residential development. Moreover, the methodology to build the GQI can be applied for efficient monitoring and management of groundwater quality in fast-growing cities with minimal prior information.

2. Materials and methods

2.1. Study area

Mongolia is one of the countries most vulnerable to climate change impacts (Batnasan, 2003; Sato et al., 2007; Garmaev et al., 2019) and has recently suffered from urbanization problems such as water scarcity and pollution of water and air (Karthe et al., 2014; Warburton et al., 2018). Ulaanbaatar is a fast-growing city, and is situated in a basin (1300 m a.s.l.) in the northeastern part of Mongolia (47°38′–48°16′N and 106°21′–107°37′E) (Fig. 1A).

2.1.1. Land use

Ulaanbaatar has developed along the Tuul River and is surrounded by high mountains in the north (Chingeltei Khairkhan, 1947 m a.s.l.) and south (Bogd Khan, 2256 m a.s.l.) (Fig. 1B). Land use in Ulaanbaatar consists mainly of natural land cover (forest and grassland) and residential areas (Fig. 1B). The natural forest areas (about 117,000 ha; 30%) are located at the southern and northern boundaries of Ulaanbaatar and include protected zones and summer camps (i.e., residential houses only for summer). The grasslands (about 241,200 ha; 61%) occur in peripheral regions and are used locally for agriculture (Tsutsumida et al., 2015; Gantumur et al., 2017). The residential area is about 317 km^2 (8%) and is divided into two zones: city center and peri-urban area. The city center represents modern built-up areas with apartments, factories, commercial buildings, schools and governmental facilities. On the other hand, the north rings of the city center are typically occupied by peri-urban districts with an area of >50% of the total residential area in Ulaanbaatar (Kamata et al., 2010; Gantumur et al., 2017).

More than 60% of the population of Ulaanbaatar live in the peri-urban area (Kamata et al., 2010; SDOU, 2015). Many residents in this area live without the benefits of basic infrastructure such as a water

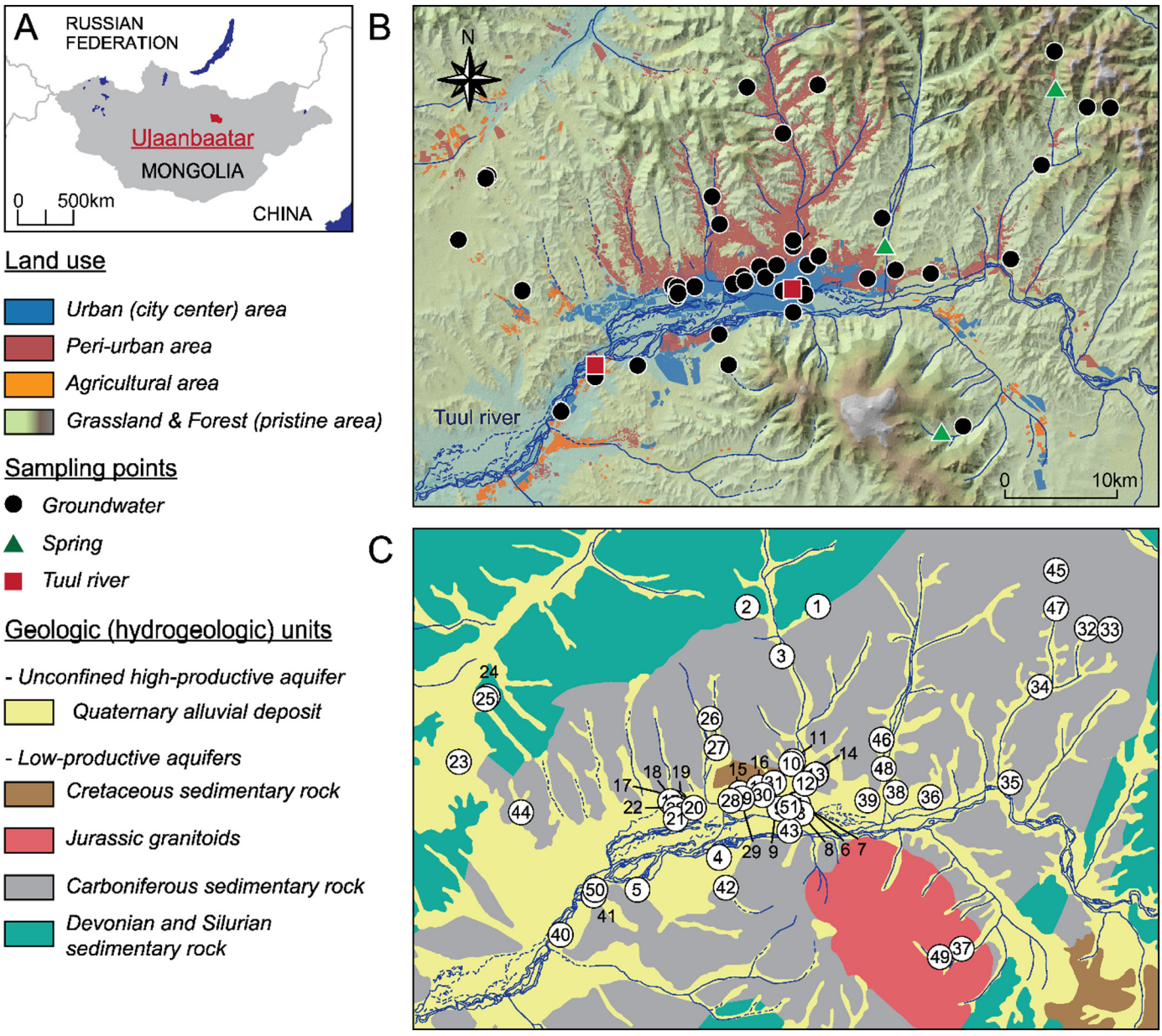

Fig. 1. Maps showing (A) the location of Ulaanbaatar in Mongolia, (B) the sampling locations for groundwater, spring, and Tuul River on land use combined with topography, and (C) the sample names on simplified geologic and hydrogeologic units in the study area. Geographical coordinates of each sampling site are provided in Supplementary Table S1.

supply system and sanitation and septic facilities (Bock, 2014; Byambadorj and Lee, 2019; Dalai et al., 2019; Munkhsuld et al., 2020). The poor sanitation of sewage including unsealed pit latrines is considered to increase the likelihood of groundwater pollution by several anthropogenic substances such as nitrate and pathogenic bacteria with the subsurface leakage and infiltration of sewage effluents (Hofmann et al., 2014; Batsaikhan et al., 2018), which imposes a potential health risk from waterborne diseases (Basandorj and Altanzagas, 2007). Therefore, it is urgently needed to assess the status of groundwater quality in Ulaanbaatar. However, only a few studies have been performed to evaluate groundwater quality; for example, Nriagu et al. (2012) on high levels of uranium, and Batsaikhan et al. (2018) on water resources sustainability.

2.1.2. Climate and geology

Ulaanbaatar is situated in a cold continental (Dwc) and cold semi-arid climate (BSk) by the Köppen climate classification, and is characterized by a harsh and cold winter, low precipitation, and large diurnal and seasonal temperature fluctuations (Sato et al., 2007). For the previous 42 years, the average monthly temperature was −26 °C in winter and 17 °C in summer, and the annual precipitation was 179 mm (Khishigjargal et al., 2014), of which nearly 74% occurred in summer months (May to August) and about 90% returned to the atmosphere by evapotranspiration. Thus, the annual water availability in Ulaanbaatar is only 4.6 l/day per capita, which is much less than the WHO standard (15–20 l/day; WHO/UNICEF, 2008). The water supply in Ulaanbaatar is largely dependent on groundwater that is extracted from shallow (30–70 m deep) boreholes ($n = 133$) in alluvial aquifers of the Tuul River basin, accounting for about 80% of the total water consumption (UNDP, 2008). People living in the city center area benefit from the main water supply system, whereas most people in peri-urban areas purchase water at water kiosks (> 550 units) or use illegal private wells (Kamata et al., 2010; UN-HABITAT, 2010; Byambadorj and Lee, 2019; Dalai et al., 2019).

The geologic setting of Ulaanbaatar is dominated by Devonian to Carboniferous sedimentary rocks that were formed as an oceanic

accretionary prism with the repetition of chert-clastic rock successions, were intruded by Jurassic to Triassic granitoids in the south, and were locally covered by Cretaceous sedimentary rocks (Kurihara et al., 2009; Takeuchi et al., 2012) (Fig. 1C). The sedimentary rock units consist mainly of siliceous shale and fine-grained silt and sandstones with intercalations of chert and coal; granitoids are mainly composed of coarse-grained porphyritic "Gorkhi" granite (Takeuchi et al., 2012; Purevjav and Roser, 2013). These basement rocks are overlain by Quaternary alluvial deposits along the Tuul River and its tributaries (Fig. 1C). The alluvial deposits (thickness: 3 to 54 m, average 20–30 m) consist mainly of permeable sand and gravel with thin interlayers of clay and silt, which form a principal aquifer for the water supply system in Ulaanbaatar (Lu and Sato, 2007; Purevjav and Roser, 2013). The aquifer is generally in an unconfined condition with transmissivities ranging from 89 to 539 m^3/m/day (United Nations, 2003). Even though the groundwater is usually encountered at shallow depths (0.5 to 4 m), some shallow groundwater wells dry up, especially from March to April (Batnasan, 2003).

2.2. Sampling and analysis

For this study, a total of 51 water samples (46 groundwater samples from private or public groundwater wells, two from the Tuul River, and three from springs) were collected by a field campaign for about 10 days in early to middle July of 2011 (wet season), covering various land uses such as grassland, forest, city center, and peri-urban residential area. Sampling locations are illustrated with land use type in Fig. 1B and geology in Fig. 1C, and are shown with geographical coordinates in Supplementary Table S1. During the sampling period, there was relatively high rainfall (32 mm total) for two days; there was also heavy rain with a cumulative amount of about 75 mm (60 mm for two days) for about half a month before sampling.

Sensitive parameters such as pH, redox potential (Eh), electrical conductivity (EC) and dissolved oxygen (DO), together with the depth to the groundwater table (if measurable), were measured in the field. A specially designed flow chamber was used to minimize contact with air when we measured the parameters using electrodes and then collected samples for subsequent laboratory analyses. All portable meters were calibrated and checked before the measurements. The alkalinity (as HCO_3^-) of water was also determined in the field by volumetric titration using 0.05 N HNO_3. In the field, the concentrations of Fe^{2+} and NH_4^+-N were also determined using a DR/890 colorimeter (HACH), as they are very sensitive to the oxidation state of water.

The collected water samples were filtered in the field with 0.45 μm membrane filters and then transferred to pre-washed 50 ml HDPE bottles for the analysis of cations, anions and stable isotopes ($\delta^{18}O$ and δ^2H of water and $\delta^{15}N$ and $\delta^{18}O$ of nitrate). Bottles for major cations analysis were acidified to pH < 2 by adding a few drops of ultrapure nitric acid. The cations (Na^+, K^+, Ca^{2+}, Mg^{2+}, Fe_{total}, Mn_{total}, Sr^{2+}) and dissolved silica (SiO_2) in water samples were analyzed using inductively coupled plasma-atomic emission spectroscopy (ICP-AES, Perkin-Elmer Optima 3000XL), while anions (Cl^-, SO_4^{2-}, NO_3^-, HCO_3^-, F^-) were determined using ion chromatography (DX-120, Dionex) at the Center for Mineral Resources Research (CMR) of Korea University following the Standard Method (APHA et al., 2001). Careful quality control of hydrochemistry data was conducted by routinely measuring blanks, duplicates and standards. The charge balances were generally below ±5%.

The oxygen isotope compositions ($\delta^{18}O$) of collected water samples were analyzed following the conventional CO_2 equilibration method (Epstein and Mayeda, 1953), while the hydrogen isotope composition (δ^2H) was measured on H_2 gas produced by the Cr reduction method using a Finnigan H-Device (Gehre et al., 1996). We used a gas-source isotope ratio mass spectrometer (Finnigan MAT 252) at the Stable Isotope Laboratory of CMR at Korea University. Analytical errors were better than ±0.05‰ for $\delta^{18}O$ and ±0.5‰ for δ^2H.

The determination of $\delta^{15}N$ and $\delta^{18}O$ values of nitrate in water samples was conducted using a Finnigan MAT Delta Plus XL isotope ratio mass spectrometer at the Isotope Science Laboratory of the University of Calgary, Canada. The samples for $\delta^{15}N$-NO_3^- analysis were prepared by following the procedure in Silva et al. (2000); nitrate was eluted with HCl and converted to $AgNO_3$ by adding Ag_2O, and the $AgNO_3$ solution was then freeze-dried to purify the $AgNO_3$ for analysis. For the $\delta^{18}O$-NO_3^- isotope analysis, nitrate oxygen was converted to CO_2 by combustion of pure $AgNO_3$ using excess graphite (Silva et al., 2000). The $\delta^{15}N$-NO_3^- values are noted in per mil deviation relative to AIR with a precision of ±0.3‰, and $\delta^{18}O$-NO_3^- is reported relative to V-SMOW with an analytical precision of ±0.5‰.

2.3. Statistical methods and thermodynamic calculations

We performed PCA to reduce the dimensionality of a multivariate dataset to two PCs and to reveal predominant patterns. Prior to the PCA analysis, the log-ratio transformation of raw data was conducted to avoid erroneous statistical effects by applying the wrong geometry or simplex (Egozcue et al., 2003; Buccianti, 2013). Specifically, we conducted PCA using the isometric log-ratio (ilr) transformation for hydrochemical parameters (Ca^{2+}, Mg^{2+}, Na^+, K^+, Sr^{2+}, SiO_2, HCO_3^-, Cl^-, SO_4^{2-}, NO_3^-) because the data did not include significant outliers. Then, the obtained PCA loadings and scores of ilr-transformed data were back-transformed to centered log-ratio (clr) values (Egozcue et al., 2003; Filzmoser et al., 2009) to examine statistically meaningful hydrochemical parameters between water samples, because the interpretations of ilr data and the statistical results are not straightforward; for easy interpretation, the ilr data are back-transformed to the clr data (Filzmoser et al., 2009). Loadings for the environmental isotopic compositions (δ^2H, $\delta^{18}O$, $\delta^{15}N$-NO_3^- and $\delta^{18}O$-NO_3^-) were obtained by the cross product of PC scores and isotopic data because they were not used for PCA.

Then the PCA results were used for compositional data analysis to suggest the GQI. Namely, the subcomposition representing groundwater contamination was analyzed. The compositional data analysis also requires log-ratio transformation to avoid spurious and misleading results in geochemical research (Buccianti, 2013; Filzmoser et al., 2010; Buccianti et al., 2014; Engle and Blondes, 2014; Engle and Rowan, 2014). Moreover, the simplex of D-part subcomposition is statistically equivalent to a D-1 dimensional Euclidean space composed of the ilr coordinates where D is the number of compositions. For example, the ilr coordinate of the three-part subcomposition, $ilr\,[x_1, x_2, x_3]$, is defined as:

$$ilr[x_1, x_2, x_3] = (z_1, z_2) = \left[\sqrt{\frac{1}{2}}\ln\frac{x_1}{x_2}, \sqrt{\frac{1}{6}}\ln\frac{x_1 \cdot x_2}{{x_3}^2}\right] \quad (1)$$

Data transformations and multivariate statistical analyses were performed using the robComposition package (Templ et al., 2011) in version 3.1.1 of R. In addition, the geochemical modelling program of PHREEQC (Parkhurst and Appelo, 1999) was used to calculate the saturation indices (SI) of water samples with respect to carbonates (calcite and dolomite) and gypsum and to create the stability diagrams for silicate mineral phases (albite, K-feldspar, Mg-saponite, anorthite, and secondary minerals) according to Morán-Ramírez et al. (2016) so as to examine the water-rock interaction affecting groundwater hydrochemistry.

3. Results

The physicochemical parameters and environmental isotopic compositions of water samples ($n = 51$) are presented in Supplementary Tables S1 and S2. Supplementary Table S3 shows a statistical summary of groundwater ($n = 46$) from wells in Ulaanbaatar.

3.1. Isotopic compositions (δ^2H and $\delta^{18}O$) of water

The δ^2H and $\delta^{18}O$ values of groundwater samples varied widely between −126.8 and −83.4‰ (median −102.4‰) and between −16.4 and −10.6‰ (median −13.2‰), respectively (Supplementary Table S3). The $\delta^{18}O$ versus δ^2H plot (Fig. 2A) shows a good linear relationship with the following equation:

$$\delta^2H = 6.7\delta^{18}O - 13.6 \left(R^2 = 0.95\right) \quad (2)$$

For comparison, the local meteoric water line (LMWL) that was suggested by Tsujimura et al. (2007a) for precipitation over the northeastern part of Mongolia (including Ulaanbaatar) is also shown in Fig. 2A, together with the global meteoric water line (GMWL; Craig, 1961). The suggested LMWL has the regression equation as follow:

$$\delta^2H = 7.5\delta^{18}O + 2.1 \quad (3)$$

The slope of the regression line for Ulaanbaatar groundwater isotopic values in Eq. (2) was lower than that of the LMWL in Eq. (3) (Fig. 2A), and in addition, the groundwater showed higher δ^2H and $\delta^{18}O$ but lower d-excess than spring and river waters (Fig. 2B).

Tsujimura et al. (2007a) and Yamanaka et al. (2007) found that i) the isotopic compositions of precipitation over northeastern Mongolia show a significant temporal (monthly and daily) fluctuation and ii) the compositions tend to show seasonal changes, which are characteristically lower in cold winter but higher in hot summer. Careful comparison of our data with such a seasonal pattern shows that the δ^2H and $\delta^{18}O$ values of groundwater in Ulaanbaatar generally agree with those of summer rainfalls. There is no doubt that the alluvial aquifer in Ulaanbaatar is predominantly recharged by summer rainfall, as nearly 74% of total precipitation in Ulaanbaatar occurs during summer months (see Section 2.1.2). The summer rainfalls in hot temperatures have high isotopes and are the major recharge source of alluvial groundwater in Ulaanbaatar.

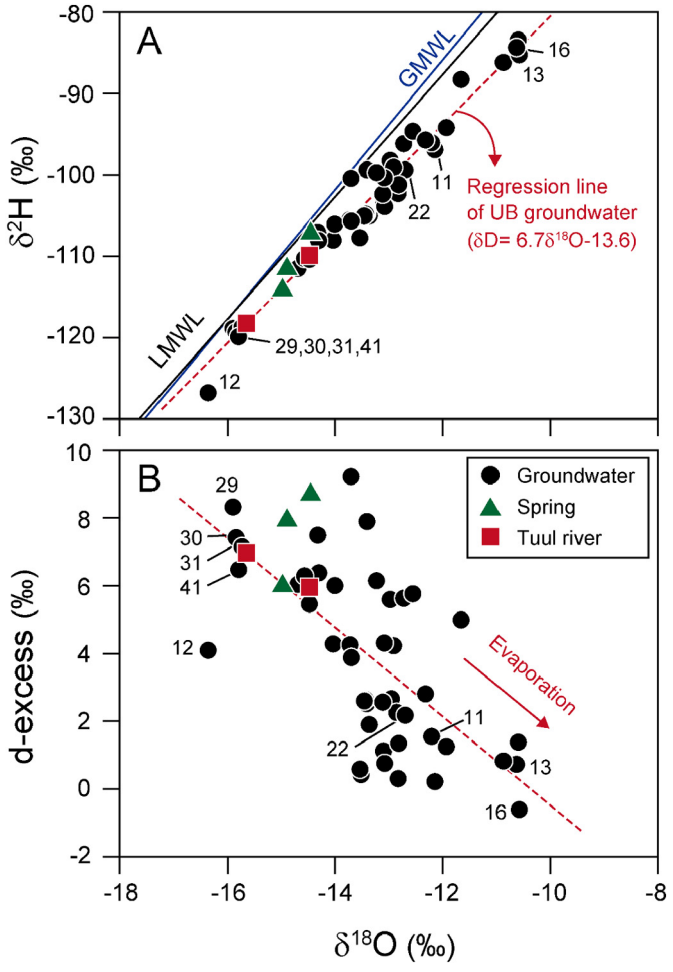

Fig. 2. (A) The stable water isotopic values (δ^2H and $\delta^{18}O$) of groundwater, spring and Tuul River samples along with GMWL (Craig, 1961) and LMWL for precipitation over northeastern Mongolia (Tsujimura et al., 2007a), and (B) the relationship between the calculated d-excess and the $\delta^{18}O$ values showing the evaporation influence on groundwater during the recharging process. UB in (A) represents Ulaanbaatar.

3.2. General hydrochemistry

The pH of Ulaanbaatar groundwater ranged from 6.7 to 8.2, with a median of 7.4, showing neutral to slightly alkaline conditions. The total dissolved solids (TDS) varied widely from 81 to 4285 mg/l, with a median of 369 mg/l (Supplementary Table S3). It is noticeable that some groundwater samples (UB-11, UB-13, UB-16, UB-22) collected from peri-urban areas had very high TDS levels exceeding the allowable limits of drinking water (1000 mg/l; WHO, 2008) in Fig. 3A, indicating significant groundwater contamination, especially in peri-urban areas.

The NO_3^- concentrations in Ulaanbaatar groundwater ranged from 1.1 to 1131.2 mg/l (median 13.7 mg/l; Supplementary Table S3), with the exceedance of the drinking water standard (> 50 mg/l; WHO, 2008) in 28% ($n = 14$) of total samples. Fig. 4A shows that highly elevated nitrate in groundwater characteristically occurs within urbanized areas (esp. peri-urban areas), whereas nitrate levels are generally low in groundwater from grassland and forest areas. In addition, the concentrations of Cl^- and SO_4^{2-} in groundwater ranged from 0.8 to 494.1 mg/l (median 15.2 mg/l) and from 5.6 to 510.6 (median 28.3 mg/l), respectively (Supplementary Table S3), and increased with TDS (Fig. 3B); for both ions, two samples (UB-16 and UB-22) exceeded the allowable limits of drinking water (> 250 mg/l; WHO, 2008).

The hydrochemical types and characteristics of water samples were examined on a Durov diagram with TDS concentrations (Fig. 3A). Most groundwater samples were classified as Ca-HCO_3 and Ca-NO_3-Cl types, while a few groundwater samples showed the relative enrichments of Mg^{2+} and Na^+ among major cations, which were classified as Mg-HCO_3 type (UB-5, UB-44, UB-24, UB-23), Mg-NO_3-Cl type (UB-16), Na-HCO_3 type (UB-15), and Na-NO_3-Cl type (UB-22) (Fig. 3A). Meanwhile, water samples from springs and the Tuul River were fresher (TDS: 52 to 137 mg/l; NO_3^-: 0.1 to 3.4 mg/l) and more alkaline (pH: 7.0–8.0) than groundwater samples, and belonged to the Ca-HCO_3 type (Fig. 3; Supplementary Table S1).

We should note that the increased TDS contents (up to >1000 mg/l; WHO, 2008) in Ulaanbaatar groundwater are closely associated with the hydrochemical change toward the dominance of NO_3^- and Cl^- among major anions (Fig. 3A); this observation indicates that anthropogenic contamination is happening in Ulaanbaatar groundwater because NO_3^- and Cl^- are well-known anthropogenic contaminants in urban groundwater (Foppen, 2002; Lee et al., 2019 and references therein). It is also noted that the degree of nitrate contamination in Ulaanbaatar groundwater is well correlated with those for Cl^- and SO_4^{2-}; these solutes as well as nitrate contribute to the increasing TDS (Fig. 3B).

3.3. Dual isotopes ($\delta^{15}N$ and $\delta^{18}O$) of NO_3^-

The $\delta^{15}N$-NO_3^- and $\delta^{18}O$-NO_3^- values ranged from 3.7‰ to 26.1‰ (median 9.2‰) and from −12.3‰ to 6.5‰ (median −1.2‰), respectively (Supplementary Table S3). Urbanized areas (esp. peri-urban areas) with elevated nitrate levels generally corresponded to spaces with high $\delta^{15}N$-NO_3^- values (Fig. 4). In contrast, groundwater samples from pristine areas in the northern and southeastern forests showed relatively depleted $\delta^{15}N$-NO_3^- values with <5 mg/l NO_3^-.

The dual $\delta^{15}N$ and $\delta^{18}O$ isotopic data of nitrate are plotted in Fig. 5, together with the approximated isotopic ranges of common nitrate

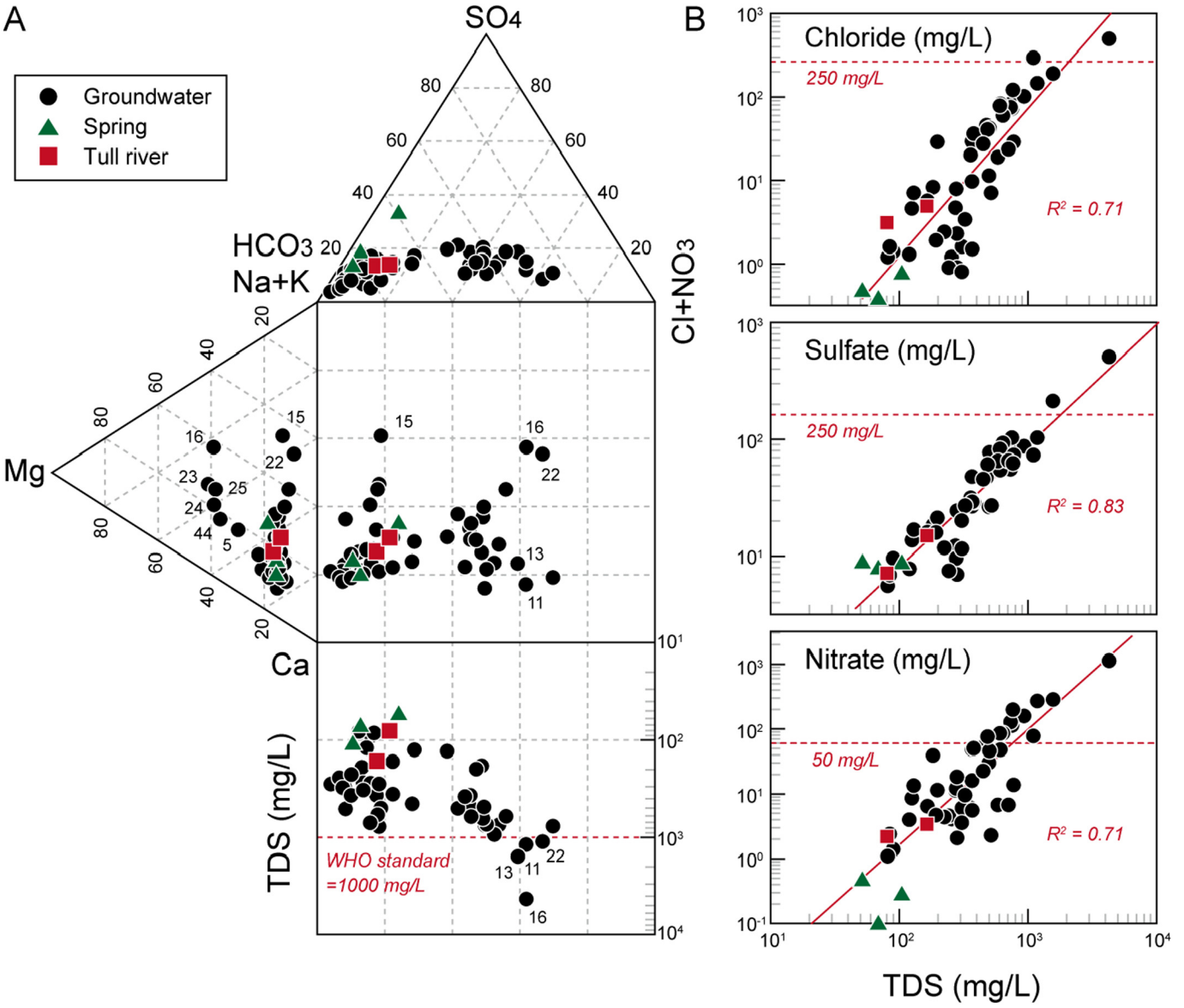

Fig. 3. (A) Durov diagram showing the hydrochemical types of water samples with total dissolved solids (TDS), and (B) the inter-relationships among TDS and anthropogenic anions (NO_3^-, Cl^- and SO_4^{2-}).

sources. All samples showed $\delta^{18}O\text{-}NO_3^-$ values below 10‰, which corresponds to those of nitrate microbially produced via nitrification during which the oxygen molecules of NO_3^- are synthesized from both H_2O and atmospheric O_2 (Kendall and Aravena, 2000; Ming et al., 2020). Accordingly, variable sources with reduced N forms, such as ammonium fertilizer, soil organic matter, manure and sewage (septic) effluent, can be considered as potential sources of NO_3^-, while atmospheric sources (even under severe atmospheric contamination in Ulaanbaatar; Amarsaikhan et al., 2014) and synthetic nitrate fertilizers have a low or negligible impact on nitrate in water bodies. Meanwhile, the $\delta^{15}N\text{-}NO_3^-$ values of Ulaanbaatar groundwater were mostly heavier than the range of nitrified ammonium fertilizers (Fig. 5), even though there were overlaps among the $\delta^{15}N\text{-}NO_3^-$ ranges from reduced N forms (Xue et al., 2009).

3.4. PCA results

A more comprehensive interpretation of the observed hydrochemical changes in Ulaanbaatar groundwater was made based on the results of a PCA bi-plot using multivariate compositional data analysis in Fig. 6A, which visualizes clr-transformed loadings for hydrochemical and isotopic parameters and scores for water samples. The first two PCs (PC1 and PC2) accounted for 63% and 13% of the total variance of examined parameters, respectively.

PC1 had high positive loadings with NO_3^-, Cl^- and $\delta^{15}N\text{-}NO_3^-$ and a negative loading with SiO_2 (Fig. 6A), indicating an increase in anthropogenic solutes (NO_3^- and Cl^-) in Ulaanbaatar groundwater along the positive direction of PC1. The loading vector of Cl^- was significantly correlated with $\delta^{15}N\text{-}NO_3^-$, while that of SiO_2 showed a cluster with HCO_3^- and alkali earth elements (Ca^{2+}, Mg^{2+}, Sr^{2+}). In PC2, K^+ typically showed the highest log-ratio variance. Also, a close relationship between nitrate concentrations and water isotopes (δ^2H and $\delta^{18}O$) was observed along the negative direction of PC2, while NO_3^- was negatively correlated with Cl^- and $\delta^{15}N\text{-}NO_3^-$ along PC2 (see Section 4.1.4).

We note that the vertices of NO_3^-, Cl^- and SiO_2 loading vectors provide the most meaningful information in the statistical context of compositional data analysis to interpret the major hydrochemical processes responsible for Ulaanbaatar groundwater (Fig. 6A). Thus, the three-part subcomposition [NO_3^-, Cl^-, SiO_2] was plotted onto a ternary diagram (i.e., simplex) to delineate major hydrochemical processes in

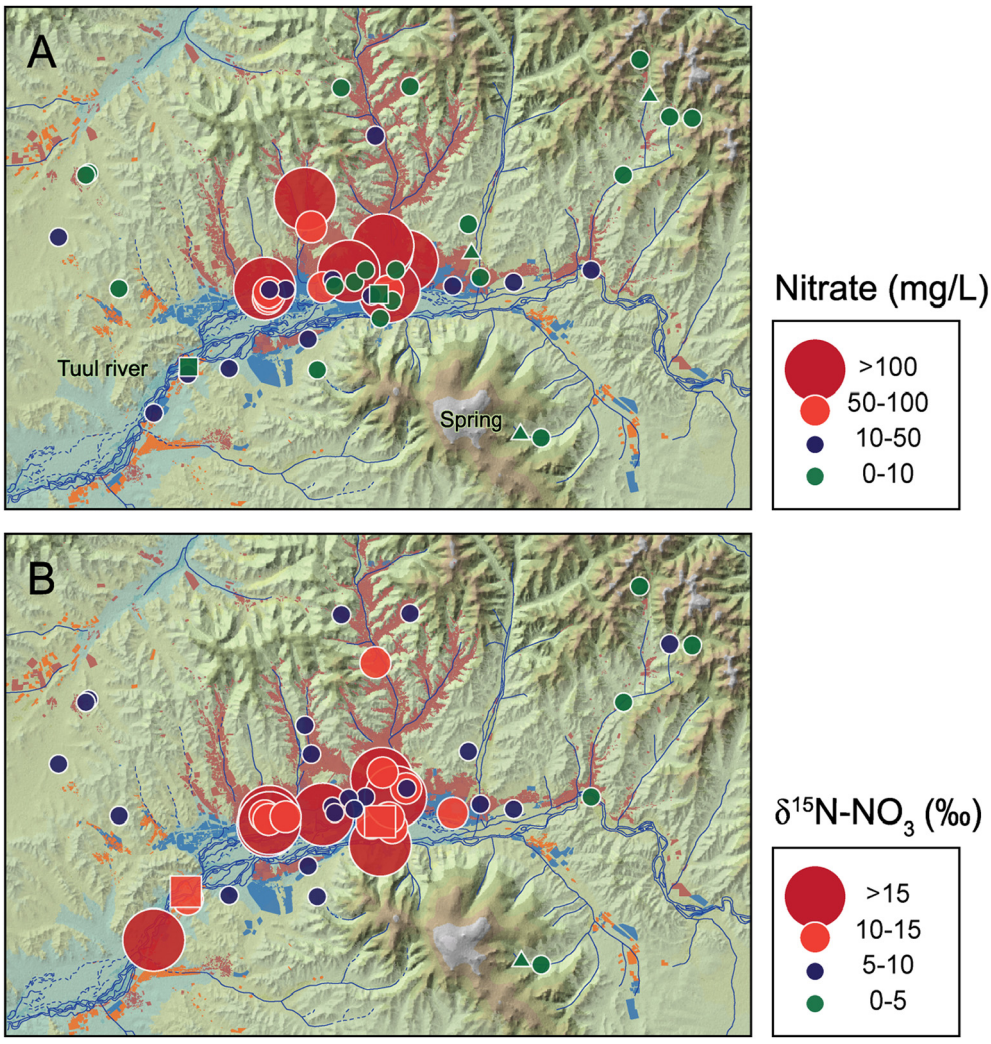

Fig. 4. Spatial distributions of NO_3^- concentrations and $\delta^{15}N\text{-}NO_3^-$ values (as shown as the symbol size) on the land use map. See the legend in Fig. 1 for land use and sample names.

Ulaanbaatar groundwater more simply and intuitively (Fig. 6B). It will be further discussed in relation to GQI in Section 4.2.

4. Discussion

4.1. Hydrochemical processes

Based on the hydrochemical, environmental isotopic and PCA results, major hydrochemical processes are discussed.

4.1.1. Anthropogenic contamination and its sources

High NO_3^-, SO_4^{2-} and Cl^- concentrations with TDS in Fig. 3B indicate the anthropogenic contamination in Ulaanbaatar groundwater. In particular, the positive loadings of NO_3^-, Cl^- and $\delta^{15}N\text{-}NO_3^-$ along PC1 indicate the groundwater nitrate contamination (Fig. 6A). The dual isotopic compositions of nitrate in Fig. 5 suggest the potential sources of nitrate as nitrified ammonium fertilizer, soil organic matter, manure, and sewage effluent. Considering the fact that the arable land in Ulaanbaatar is too small (only 2.7% of the study area; see Fig. 1B) to contribute to the production of nitrate in water, the $\delta^{15}N\text{-}NO_3^-$ ranges in all samples can now be interpreted to reflect the mixtures between the remaining sources excluding the ammonium fertilizer. Furthermore, livestock manure can be excluded because there are no massive livestock farms in both urban and peri-urban areas since most of the farm animals in Mongolia graze on grassland. Natural organic matter also cannot be considered a major contributor to the remarkable nitrate in Ulaanbaatar

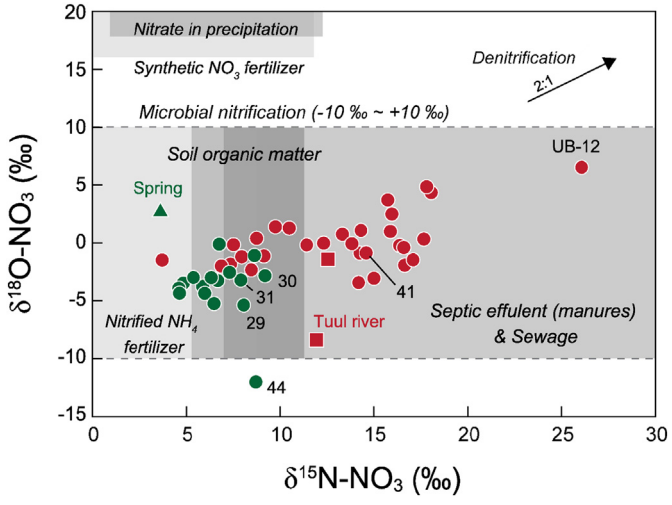

Fig. 5. The dual isotopic ($\delta^{15}N$ and $\delta^{18}O$) values of nitrate on the approximated isotopic ranges of common nitrate sources (Xue et al., 2009). Water samples are divided into Group I (baseline quality; green) and II (anthropogenic contamination; red) based on Fig. 7. The triangle and square represent the spring and Tuul River, respectively. (For interpretation of the references to color in this figure legend, the reader is referred to the web version of this article.)

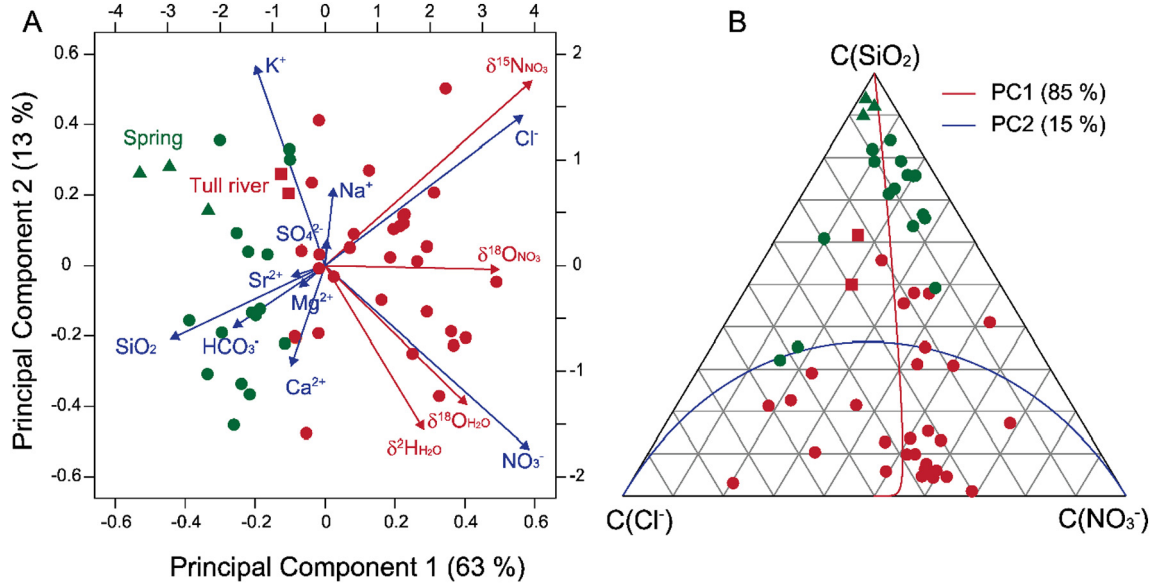

Fig. 6. (A) PCA bi-plot showing the centered log-ratio (clr) transformed scores (top and right) of water samples and loadings (bottom and left) of hydrochemical (blue arrows) and isotopic (red arrows) parameters for the first two components for the isometric log-ratio (ilr) transformed data, and (B) a ternary diagram for the subcomposition (NO_3^-, Cl^-, and SiO_2). Water samples are divided into Group I (baseline quality; green) and II (anthropogenic contamination; red) based on Fig. 7. The triangle and square represent the spring and Tuul River, respectively. (For interpretation of the references to color in this figure legend, the reader is referred to the web version of this article.)

groundwater because natural background levels of NO_3^- in soil water are very low (< 5 mg/l; Böhlke, 2002). Consequently, sewage effluent seems to be the major nitrate source in Ulaanbaatar groundwater.

Additionally, the high correlation of increased TDS contents (up to >1000 mg/l) with the hydrochemical change toward the dominance of NO_3^- and Cl^- (Fig. 3A) indicates that anthropogenic contamination is mainly due to the influx of latrine and sewage effluents because NO_3^- and Cl^- are typical inorganic pollutants derived from industrial or municipal sewage in cities (Foppen, 2002; Lee et al., 2019 and references therein). The high variability of major cations in such NO_3^- and Cl^--rich groundwater (Fig. 3A) also reflects the role of sewage effluents as a main anthropogenic source, since municipal sewage sources have variable cation ratios according to different source materials such as food waste and human feces (Foppen, 2002); of course, geogenic cations derived from the dissolution of carbonate and silicate minerals may overlap the certain amounts of cations from sewage sources (see Section 4.1.2). A high correlation of SO_4^{2-} with TDS (Fig. 3B) also supports the sewage sources because sulfate enrichments from sewage sources were reported in many urban groundwater areas (Hosono et al., 2011; Jurado et al., 2013; Lee et al., 2019).

Moreover, the spatial distribution of $\delta^{15}N\text{-}NO_3^-$ values and NO_3^- concentrations on the land use map in Fig. 4 indicate the land use control of nitrate contamination. The elevated nitrate levels with high $\delta^{15}N\text{-}NO_3^-$ values in urbanized areas (esp. peri-urban areas) suggest that significant nitrate contamination in Ulaanbaatar is largely due to sewage (pit latrine) effluents in and from peri-urban areas, which generally increase both nitrate levels and $\delta^{15}N\text{-}NO_3^-$ values, as shown in Fig. 7. Also, the loading vector of Cl^- significantly correlated with $\delta^{15}N\text{-}NO_3^-$ in Fig. 6A implies the impact of sewage on groundwater because sewer leakage contains high levels of Cl^- (Lee et al., 2019 and references therein). In contrast, one spring water sample (UB-49; 0.5 mg/l NO_3^-; triangle in Figs. 4B and 5) and groundwater samples (< 5 mg/l NO_3^-) from the pristine area showed the likely source of nitrate to be soil organic matter (Figs. 4 and 5).

Therefore, we now consider that significant nitrate contamination in Ulaanbaatar groundwater is mainly due to the leakage of untreated municipal sewage effluent including pit latrine leakage in peri-urban areas. The $\delta^{15}N\text{-}NO_3^-$ values (> 10‰) of Tuul River water samples (2.2 and 3.4 mg/l NO_3^-) indicate the source of nitrate from sewage effluent discharged into the river from urban areas (Figs. 5 and 7) as in Shi et al. (2019), although the observed chemistry of Tuul River water was diluted by freshwater discharge from upstream without significant anthropogenic sources during our sampling period. Meanwhile, springs in forest (mountain) areas possibly reflect the geochemical baseline of Ulaanbaatar groundwater that is not or is less influenced by anthropogenic disturbances (Fig. 7).

Based on the combined interpretation of NO_3^- concentrations and $\delta^{15}N\text{-}NO_3^-$, Ulaanbaatar groundwater is divided into two groups by nitrate concentration (10 mg/l) and $\delta^{15}N\text{-}NO_3^-$ value (10‰) in Fig. 7: a natural or baseline quality group (Group I; NO_3^- < 10 mg/l and $\delta^{15}N\text{-}NO_3^-$ < 10‰) and an anthropogenically contaminated group (Group II; NO_3^- ≥ 10 mg/l or $\delta^{15}N\text{-}NO_3^-$ ≥ 10‰). These two groups are significantly different for NO_3^- and $\delta^{15}N\text{-}NO_3^-$ ($p < 0.05$; Table 1). The concentration levels of some other ions (e.g., Cl^- and SO_4^{2-}) are also different between the two groups (bold in Table 1), indicating their remarkable

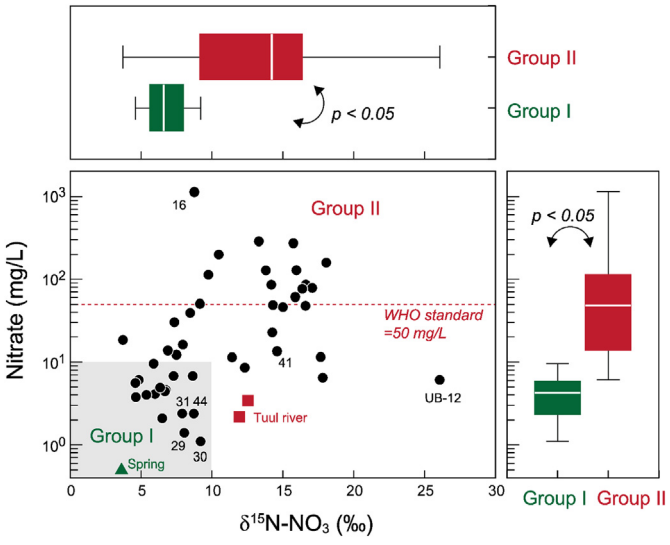

Fig. 7. Relationship between NO_3^- concentrations and $\delta^{15}N\text{-}NO_3^-$ values, from which the groundwater samples are divided into two groups (Group I: baseline quality and Group II: anthropogenic contamination). The triangle and square represent the spring and Tuul River, respectively.

Table 1
Statistical summary of physicochemical and environmental isotopic data of two groups of groundwater samples, Ulaanbaatar City, Mongolia. The p–values indicate the statistical difference between the two groups; bold characters denote the significant difference ($p < 0.05$). For comparison, the averages for spring and river water are also shown. The spring and river samples belong to Group I and II, respectively in Fig. 7.

Parameters	Group I (natural; defined by NO_3^- < 10 mg/l and δ^{15}N-NO_3^- < 10‰; $N = 16$)			Group II (contaminated; defined by NO_3^- ≥ 10 mg/l or δ^{15}N-NO_3^- ≥ 10‰; $N = 30$)			*p*-Value	Spring ($N = 3$)	River ($N = 2$)
	Min.	Max.	Median	Min.	Max.	Median		Mean	Mean
pH	6.8	8.2	7.5	6.7	8.1	7.3	0.42	7.5	7.8
Eh (mV)	43	485	191	53	416	175	0.92	188	149
DO (mg/l)	0.8	6.7	5.5	0.7	9.7	4.3	0.89	5.3	4.2
EC (μS/cm)	32	427	138	75	3100	373	**0.00**	53	106
TDS (mg/l)	51.8	708.1	243.0	80.5	4285.2	481.7	**0.00**	75.3	122.5
Ca^{2+} (mg/l)	6.2	67.6	42.5	12.1	338	72.7	**0.00**	11.9	20.0
Mg^{2+} (mg/l)	1.5	49.6	6.3	1.9	321.6	13.3	**0.03**	2.1	3.5
Na^+ (mg/l)	1.9	42.4	7.8	4.6	466	23.2	**0.00**	3.0	5.9
K^+ (mg/l)	0.4	5.7	0.8	0.5	9.1	2.5	**0.00**	0.7	1.8
Sr^{2+} (mg/l)	0.0	2.2	0.3	0.1	10.3	0.8	0.06	0.1	0.2
SiO_2 (mg/l)	8.2	20.2	14.0	7.1	23.5	14.0	0.86	10.2	8.4
HCO_3^- (mg/l)	16.8	437.8	151.0	39.7	1083	180	0.29	36.8	64.8
Cl^- (mg/l)	0.4	23.6	1.4	2.3	494.1	32.7	**0.00**	0.6	4.0
SO_4^{2-} (mg/l)	5.6	65.8	11.5	7.2	511	47.7	**0.00**	8.9	11.1
NO_3^- (mg/l)	0.1	9.6	4.0	2.2	1130	47.1	**0.00**	0.3	2.8
F^- (mg/l)	< 0.005	2.3	0.07	< 0.005	1.07	< 0.005	**0.00**	0.33	< 0.005
Fe^{2+} (mg/l)	< 0.01	0.3	0.02	< 0.01	0.3	0.02	0.78	0.02	0.01
Fe_{total} (mg/l)	< 0.005	0.8	< 0.005	< 0.005	0.08	< 0.005	0.76	0.03	0.03
Mn_{total} (mg/l)	< 0.001	0.6	< 0.001	< 0.001	5.4	< 0.001	0.40	< 0.001	0.01
NH_4-N (mg/l)	< 0.005	0.4	< 0.005	< 0.005	4.2	< 0.005	0.83	0.02	0.14
δ^2H-H_2O (‰)	−119	−88	−106	−127	−83	−102	0.83	−111	−114
δ^{18}O-H_2O (‰)	−15.9	−11.7	−13.7	−16.4	−10.6	−13.1	0.33	−14.8	−15.1
d-Excess (‰)	1.2	8.9	6.0	−0.6	9.2	2.6	**0.00**	7.7	6.5
δ^{15}N-NO_3^- (‰)	3.6	9.2	6.5	3.7	26.1	14.0	**0.00**	3.6[a]	12.3
δ^{18}O-NO_3^- (‰)	−12.3	2.6	−3.3	−8.4	6.5	−0.2	**0.00**	2.6[a]	−4.9

Abbreviations: DO = dissolved oxygen; Eh = redox potential; TDS = total dissolved solids.
[a] $N = 1$.

enrichments in Group II water due to the effect of untreated sewage (and pit latrine) effluents. Note that there is less variation of δ^{15}N-NO_3^- in Group I, while there is more scattered δ^{15}N-NO_3^- in Group II, which implies different degrees of nitrate contamination in Group II water.

4.1.2. Water-rock interactions

Groundwater samples with low TDS values are generally Ca-HCO_3 and Mg-HCO_3 types (Fig. 3A), which were observed in grassland and/or forest areas (Fig. 1B); these groundwater samples reflect pristine hydrochemistry that is largely controlled by the dissolution of carbonates in alluvium and soil. In particular, the relative increase in Mg^{2+} in a few baseline quality groundwater samples (UB-5, UB-44, UB-24, UB-23) can be explained by their unique geologic and geochemical control, since those samples are spatially distributed in the western grasslands of Ulaanbaatar where the basement geologic unit is different from the other sampling locations and is characteristically sedimentary rocks of Silurian to Devonian age (see Fig. 1C). Also, the clustering of SiO_2 with HCO_3^-, Ca^{2+}, Mg^{2+} and Sr^{2+} along the negative direction of PC1 (Fig. 6A) and the geology in the study area (Fig. 1C) imply the weathering of natural carbonates. Silicate weathering can also be considered to control the natural groundwater chemistry since most of

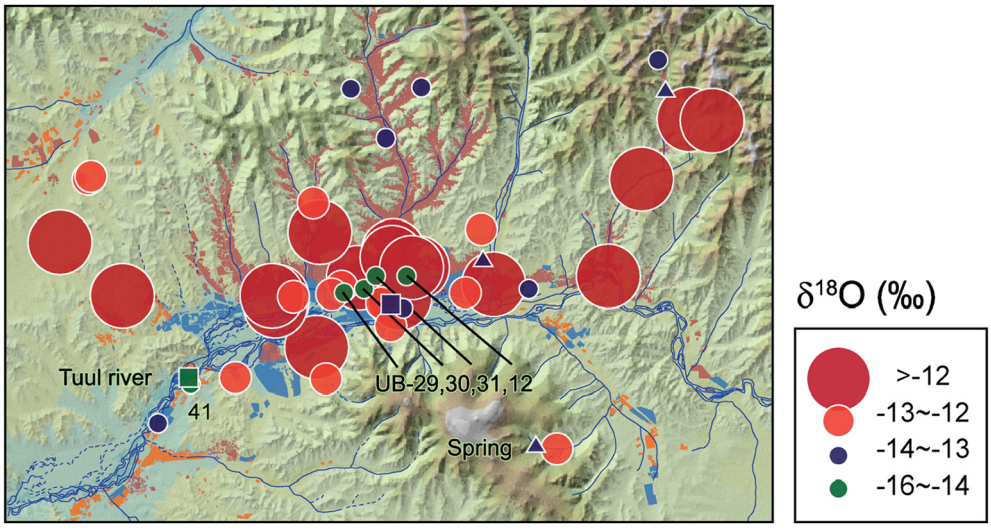

Fig. 8. Spatial distribution of the δ^{18}O values of H_2O (as shown as the symbol size) in groundwater, spring, and Tuul River water samples on the land use map. See the legend in Fig. 1 for land use.

the groundwater samples were higher in SiO_2 concentrations (median 14.3 mg/l; Supplementary Table S3) than spring and river water samples (Table 1; Supplementary Table S1).

Natural water-rock interactions also take place in groundwater contaminated with nitrate (Group II), and are sometimes enhanced by nitrification (Kim et al., 2019). In fact, most of Ulaanbaatar groundwater samples were undersaturated with respect to carbonate minerals and gypsum in both Group I and II, while some were oversaturated with calcite minerals (Supplementary Fig. S1). This indicates that the dissolution of carbonate minerals affects the hydrochemistry regardless of anthropogenic contamination. In addition, the thermodynamic stability diagrams for silicate minerals showed that most of the groundwater samples were plotted in the stability field of kaolinite irrespective of anthropogenic contamination (Supplementary Fig. S2), which implies that water-silicate rock interaction naturally occurs in Ulaanbaatar groundwater to form secondary minerals such as kaolinite. Thus, it is suggested that rainwater infiltrating with soil CO_2 seems to react with silicate minerals (e.g., plagioclase and K-feldspar) in the aquifer, naturally leaching out Na^+, K^+, Ca^{2+}, Mg^{2+} and HCO_3^- and forming kaolinite and silica. However, a more detailed investigation of the relative contribution of natural processes to the hydrochemistry remains for future work.

4.1.3. Evaporation

The evaporation process also seems to influence water infiltrated through the unsaturated zone and leads to an isotopic enrichment of the residual soil water by kinetic isotope fractionation, and consequently the isotopic signatures of evaporation (i.e., high $\delta^{18}O$ values and low d-excesses) in alluvial groundwater in Ulaanbaatar (Clark and Fritz, 1997; Tsujimura et al., 2007a; Choi et al., 2010) given that nearly 90% of annual precipitation returns to the atmosphere by evapotranspiration in the study area (see Section 2.1.2). Also, the groundwater samples collected from peri-urban areas and with high TDS levels (i.e., UB-11, UB-13, UB-16, UB-22) had high $\delta^{18}O$ and δ^2H isotopic compositions (Fig. 2), which indicates that evaporation during groundwater recharge also results in the enrichment of solute concentrations, as in Oiro et al. (2018) who found that groundwater quality was modified by increasing groundwater mineral concentration and enriching groundwater with heavy isotopes through the effect of evaporative fractionation.

Furthermore, the evaporation patterns ($\delta^{18}O$ values and d-excesses) recognized in Fig. 2B are highly variable among groundwater samples. These patterns indicate that the recharging water from the unsaturated zone experiences varying degrees of evaporation, and the alluvial aquifer in Ulaanbaatar represents a mixture of recharging water with varying degrees of evaporation. In semi-arid and arid climate regions like Ulaanbaatar, the evaporation during recharge is often observed including northeastern Mongolia (Tsujimura et al., 2007a, 2007b), and the evaporation loss of recharging water with kinetic isotope fractionation is augmented as the recharge rate (or recharge amount) decreases (Clark and Fritz, 1997). The groundwater recharging process can be understood by carefully considering the isotopic signature of recharging water that often remains in groundwater (Dogramaci et al., 2012).

In this regard, the positive direction of PC2 addresses the enrichment of solute concentrations due to evaporation during groundwater recharge in groundwater samples with high $\delta^{18}O$ and δ^2H isotopic compositions and nitrate concentrations (i.e., UB-11, UB-13, UB-16, UB-22) in Fig. 6A, whereas the close relationship between nitrate concentrations and water isotopes (δ^2H and $\delta^{18}O$) along the negative direction of PC2 and the areas of groundwater with low evaporation signatures (low $\delta^{18}O$ values and high d-excesses) may indicate different recharge processes (e.g., preferential flow or river water infiltration; see Section 4.1.4), as is found in a few localities in the northern and southern mountain areas of Ulaanbaatar (see Figs. 2 and 8). Three samples from perennial springs in the mountain area also showed low evaporation signatures (triangles in Figs. 2 and 8).

However, we should note that further studies on the altitude effect of rainfall falling over the mountain areas and on the evaporation effect considering the depths to water tables in mountain areas are needed (Gat, 1996; Gonfiantini et al., 2001). Moreover, the low d-excess is not only a signature of evaporation during rainfall recharge but also caused by a mixing with other recharge sources (e.g., urban runoff, irrigation water, artificial recharge, leakage from streams or ponds) affected by evaporation, which remains for future work.

4.1.4. River water infiltration versus denitrification

Some groundwater samples (UB-12, UB-29, UB-30, UB-31 and UB-41 in Figs. 2A and 8) collected from wells located near the Tuul River and city center showed significantly depleted water isotopic values, similar to those of the samples from the Tuul River (squares in Fig. 8 for localities). These samples can be considered to be influenced by river water infiltration with a low or negligible effect of evaporation (De Vries and Simmers, 2002; Kong et al., 2019), possibly due to groundwater level decline enhanced by the overuse of this water resource and permeable sand and gravel in the alluvial aquifer (see Section 2.1.2).

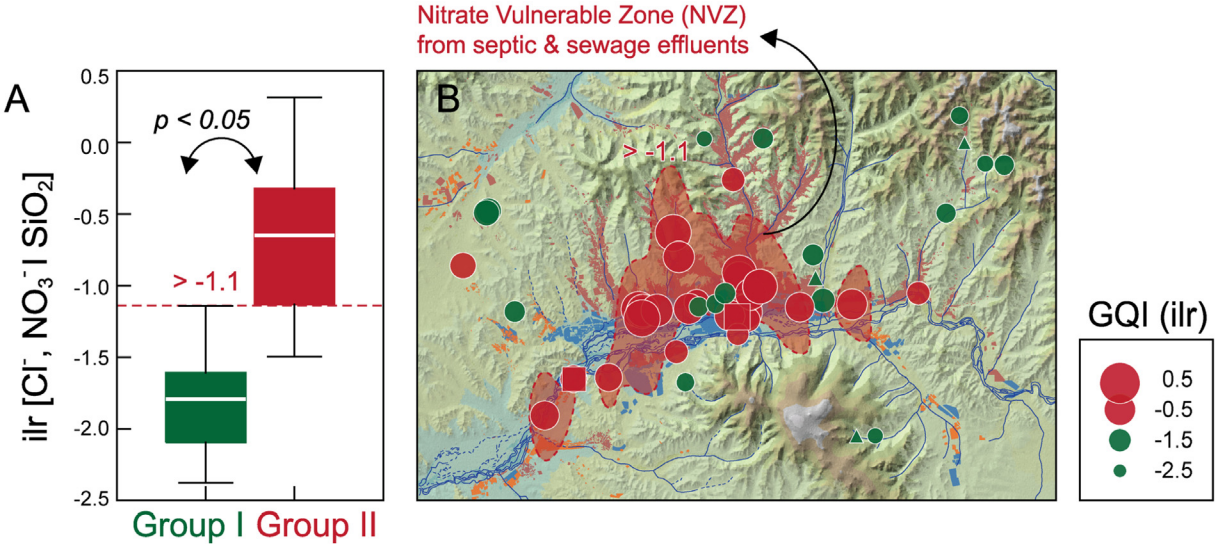

Fig. 9. (A) Box plot showing the significant difference of Groundwater Quality Index (GQI) between Group I and Group II in Fig. 7, and (B) the spatial distribution of GQI in which highly vulnerable zones are depicted by a threshold (> −1.1).

Among the alluvial groundwater samples with significantly depleted $\delta^{18}O$ and $\delta^{2}H$ isotopic values and reflecting the effect of river water infiltration, a sample (UB-12) collected near the Tuul River showed considerably high $\delta^{15}N$ and $\delta^{18}O$ values of NO_3^- (Fig. 5). The low NO_3^- concentration (6.1 mg/l) but very high $\delta^{15}N$ and $\delta^{18}O$ values of nitrate for the sample may be attributed to denitrification (Fukada et al., 2003; Itoh et al., 2011) which can occur during the hyporheic exchange between river and groundwater in riparian zones of riverside alluvial aquifers (Mengis et al., 1999). Also, NO_3^- is negatively correlated with Cl^- and $^{15}N\text{-}NO_3^-$ along PC2 in Fig. 6A, implying denitrification.

However, denitrification cannot successfully explain the observed data for the other three samples (UB-29, UB-30, UB-31) collected near the city center alongside the Tuul River (see Fig. 8 for localities). Even though these three samples were very low in NO_3^- concentrations (1.1 to 2.4 mg/l) and also had very depleted $\delta^{18}O$ and $\delta^{2}H$ isotopic values approaching those of Tuul River water (see Fig. 2A), their indiscernible enrichments of both $\delta^{15}N\text{-}NO_3^-$ (7.9 to 9.2‰) and $\delta^{18}O\text{-}NO_3^-$ (−5.4 to −2.8‰) in Fig. 5 cannot be explained solely by denitrification. Alternatively, the dilution of contaminated groundwater by river water infiltration can be an explanation for the observation (Fig. 7). Thus, it can be summarized that groundwater recharge in Ulaanbaatar occurs mainly through rainwater infiltration during summer based on the $\delta^{18}O$ and $\delta^{2}H$ isotopic compositions of shallow (< 70 m deep) groundwater in Fig. 2, while it is also locally influenced by river water infiltration near the Tuul River. Better understanding of the interaction between river water and groundwater using environmental isotopic compositions remains for future studies.

4.2. Groundwater Quality Index (GQI)

Based on the major hydrochemical processes, i.e., anthropogenic contamination and natural process by PC1 and evaporation and river infiltration by PC2, PCA results show a good separation between anthropogenic and natural impacts on Ulaanbaatar groundwater, especially by PC1 (Fig. 6A). Moreover, the baseline quality versus contaminated groups are well separated by the proportional increases in NO_3^- and Cl^- and the proportional decrease in SiO_2 (Fig. 6B); this feature, explained by PC1, accounts for 85% of the total variances of PC1 and PC2. Thus, the log-ratio variances of the subcomposition [NO_3^-, Cl^-, SiO_2] can be used to evaluate groundwater quality degradation (i.e., nitrate contamination due to sewage (pit latrine) sources in peri-urban areas) without the loss of information.

Among the ilr coordinates of the three-part subcomposition in Eq. (1), z_2 agrees well with the PC1 axis consisting of all three variables, and can be used to build up a simple hydrochemical index to comprehensively evaluate and monitor the impact on Ulaanbaatar groundwater by anthropogenic processes. Thus, we suggest z_2 in Eq. (1) as the GQI in the following equation:

$$GQI = \sqrt{\frac{1}{6}} \ln \frac{[NO_3^-][Cl^-]}{[SiO_2]^2} \quad (4)$$

where the concentration unit is mg/l.

The respective GQI scores for Ulaanbaatar groundwater samples are shown as a spatial map (Fig. 9B). Furthermore, the nitrate vulnerable zone (NVZ) is also delineated to show the area of strong septic and sewage (pit latrine) impacts on Ulaanbaatar groundwater; for the areal delineation, we used ordinary kriging and a threshold (> −1.1) for the GQI score. The threshold was defined by the highest GQI value in Group I water (Fig. 9A).

We acknowledge that an index should include land use and hydrogeology data as well as hydrochemical data to better assess groundwater quality, as in DRASTIC (Depth to water, Recharge, Aquifer media, Soil media, Topography, Impact of vadose zone media, and Hydraulic conductivity; Khosravi et al., 2018). However, fast-growing cities do not have enough information to characterize land use or hydrogeology. Another advantage of the suggested GQI score is the cost-effective monitoring (i.e., simple analyses of NO_3^-, Cl^- and SiO_2) of groundwater quality degradation by poor sanitary facilities in Ulaanbaatar and other poorly developed urban areas.

5. Conclusions and suggestions

Ulaanbaatar, the capital of Mongolia, is in a semi-arid region and represents a city quickly urbanizing by massive rural-to-urban migration and therefore facing significant environmental concerns, especially the degradation of the quantity and quality of groundwater due to unsewered residential development. Special concern has been paid to peri-urban areas without basic infrastructure such as sanitation and septic facilities. Thus, this study was performed to evaluate groundwater quality in relation to land use in Ulaanbaatar by the combined interpretation of hydrogeochemical and environmental isotopic ($\delta^{18}O$ and $\delta^{2}H$ of water and $\delta^{18}O$ and $\delta^{15}N$ of nitrate) data in conjunction with a multivariate compositional data analysis approach. The roles of natural and anthropogenic processes in controlling groundwater chemistry were also examined.

Based on the hydrochemical, environmental isotopic and PCA results, four major hydrogeochemical processes can be identified in the study area: groundwater contamination from sewage and septic effluents and water-rock interaction addressed by PC1, and evaporation during groundwater recharge and river water infiltration with low or negligible evaporation addressed by PC2, even though the current dataset is not sufficient to make a clear statement. Ulaanbaatar groundwater shows clear land use control: highly polluted in the urban center and peri-urban areas, while in a natural state (i.e., baseline) in grassland and forest areas. Groundwater in urbanized areas is highly contaminated by nitrate (and Cl^-, SO_4^{2-} and TDS), with the exceedance of the WHO drinking water standard for nitrate in 28% of total samples. From the results of a PCA bi-plot using multivariate compositional data analysis, we suggest a Groundwater Quality Index (GQI) with the concentrations of NO_3^-, Cl^- and SiO_2, which is used for delineating areas with strong septic and sewage (pit latrine) impacts on Ulaanbaatar groundwater.

We acknowledge that our data are from 2011 and represent only one sampling season and, as Ulaaanbaatar has grown rapidly, the current states of groundwater contamination in the city may have changed slightly over the past about 10 years even though residents in peri-urban areas still live without the benefits of basic infrastructure such as sanitation and septic facilities. Even so, the results of this study may provide a reference for future research on groundwater quality in regions that are in the early growing stages of urbanization; for example, studies on the time gap between land use change and groundwater contamination, due to legacy nitrogen, not only in the study area but also in other rapidly growing cities without basic infrastructure in peri-urban areas. The study results can also be used to suggest adequate controls for groundwater pollution. For instance, the highly contaminated groundwater in urbanized areas of Ulaanbaatar, especially in highly populated peri-urban areas without municipal sanitation facilities, may have an impact on the public health risks associated with groundwater sources. Therefore, it is urgently needed to facilitate a new policy to improve environmental sanitation, as has been established in 2013 by the Ulaanbaatar Municipality as the “Ger Area Redevelopment Programme (GARP)” based on the Master Plan 2030. Public campaigns on the effects of contaminated water and dangers of the use of illegal groundwater wells close to pit latrines should be more widespread. As indicated by this study, substantial improvement of pit latrines and sewage systems in peri-urban areas is critical. In a scientific context, it is necessary to determine and regulate the distance from groundwater wells to pit latrines. Along with a more in-depth understanding of the groundwater system in Ulaanbaatar, a systematic monitoring system should be established to evaluate the status of groundwater. For this purpose, a simple hydrochemical index such as the GQI referred to in

this study can be useful in a fast-growing city with little information on land use or hydrogeology.

CRediT authorship contribution statement

Bayartungalag Batsaikhan: Methodology, Formal analysis, Investigation, Visualization, Writing - original draft. **Seong-Taek Yun:** Conceptualization, Methodology, Writing - review & editing, Supervision, Project administration, Funding acquisition. **Kyoung-Ho Kim:** Conceptualization, Methodology, Formal analysis, Visualization, Writing - original draft. **Soonyoung Yu:** Formal analysis, Validation, Data curation, Writing - review & editing. **Kyung-Jin Lee:** Investigation, Software, Validation. **Young-Joon Lee:** Investigation, Project administration. **Jadambaa Namjil:** Investigation, Resources, Writing - review & editing.

Declaration of competing interest

The authors declare that they have no known competing financial interests or personal relationships that could have appeared to influence the work reported in this paper.

Acknowledgements

This study was initially supported by the Korea Environment Institute (KEI) and was prepared for a doctoral thesis by the first author in February 2017. The completion of this study was supported from Korea Environmental Industry & Technology Institute (KEITI) through the Subsurface Environment Management (SEM) Project, funded by the Korea Ministry of Environment (MOE) (2018002440002). Dr. Ariunzul Yangiv helped us with field work for hydrogeologic knowledge. The comments and suggestions from four anonymous reviewers have helped to improve and clarify this manuscript.

Appendix A. Supplementary data

Supplementary data to this article can be found online at https://doi.org/10.1016/j.scitotenv.2020.142790.

References

Amarsaikhan, D., Battsengel, V., Nergui, B., Ganzorig, M., Bolor, G., 2014. A study on air pollution in Ulaanbaatar City, Mongolia. J. Geosci. Environ. Protec. 2, 123–128. https://doi.org/10.4236/gep.2014.22017.

APHA, AWWA, WEF, 2001. Standard Methods for the Examination of Water and Wastewater. American Public Health Association, Washington DC.

Bao, C., Fang, C.L., 2007. Water resources constraint force on urbanization in water deficient regions: a case study of the Hexi Corridor, arid area of NW China. Ecol. Econ. 62, 508–517.

Barrett, M.H., Howard, A.G., 2002. Urban groundwater and sanitation - developed and developing countries. Current Problems of Hydrogeology in Urban Areas, Urban Agglomerates and Industrial Centres. Springer.

Basandorj, D., Altanzagas, B., 2007. Current situation and key problems on water supply and sanitation in Mongolia. Proceedings of the International Forum on Strategic Technology, Ulaanbaatar http://ieeexplore.ieee.org/stamp/stamp.jsp?tp=&arnumber=4798550.

Batnasan, N., 2003. Freshwater issues in Mongolia. Proceeding of the National Seminar on IRBM in Mongolia, 24-25 Sept. 2013, Ulaanbaatar, pp. 53–61.

Batsaikhan, N., Lee, J.M., Nemer, B., Woo, N.C., 2018. Water resources sustainability of Ulaanbaatar City, Mongolia. Water 10, 750. https://doi.org/10.3390/w10060750.

Bayanchimeg, Ch., Batbayar, B., 2013. The population and economic activity of Ulaanbaatar. ERINA Report, No. 109 , pp. 62–67. https://www.erina.or.jp/wp-content/uploads/2013/01/se10981_tssc.pdf.

Bock, F., 2014. Water Supply, Sanitation and Hygiene in Mongolia: An Institutional Analysis. ACF Mongolia, Ulaanbaatar https://doi.org/10.13140/2.1.1641.7288.

Böhlke, J.K., 2002. Groundwater recharge and agricultural contamination. Hydrogeol. J. 10, 153–179.

Buccianti, A., 2013. Is compositional data analysis a way to see beyond the illusion? Comput. Geosci. 50, 165–173.

Buccianti, A., Nisi, B., Martín-Fernández, J.A., Palarea-Albaladejo, J., 2014. Methods to investigate the geochemistry of groundwaters with values for nitrogen compounds below the detection limit. J. Geochem. Explor. 141, 78–88.

Byambadorj, A., Lee, H.S., 2019. Household willingness to pay for wastewater treatment and water supply system improvement in a Ger area in Ulaanbaatar City, Mongolia. Water 11, 1856. https://doi.org/10.3390/w11091856.

Byambadorj, T., Amati, M., Ruming, K.J., 2011. Twenty-first century nomadic city: ger districts and barriers to the implementation of the Ulaanbaatar City Master Plan. Asia Pac. Viewp. 52, 165–177.

Chambers, L.G., Chin, Y.P., Filippelli, G.M., Gardner, C.B., Herndon, E.M., et al., 2016. Developing the scientific framework for urban geochemistry. Appl. Geochem. 67, 1–20.

Choi, B.Y., Yun, S.T., Mayer, B., Chae, G.T., Kim, K.H., Kim, K., Koh, Y.K., 2010. Identification of groundwater recharge sources and processes in a heterogeneous alluvial aquifer: results from multi-level monitoring of hydrochemistry and environmental isotopes in a riverside agricultural area in Korea. Hydrol. Process. 24, 317–330.

Clark, I.D., Fritz, P., 1997. Environmental Isotopes in Hydrogeology. CRC Press.

Craig, H., 1961. Isotopic variations in meteoric waters. Science 133, 1702–1703.

Dalai, S., Dambaravjaa, O., Purevjav, G., 2019. Water challenges in Ulaanbaatar, Mongolia. In: Ray, B., Shaw, R. (Eds.), Urban Drought. Disaster Risk Reduction (Methods, Approaches and Practices). Springer, Singapore.

De Vries, J.J., Simmers, I., 2002. Groundwater recharge: an overview of processes and challenges. Hydrogeol. J. 10, 5–17.

Dogramaci, S., Skrzypek, G., Dodson, W., Grierson, P.F., 2012. Stable isotope and hydrochemical evolution of groundwater in the semi-arid Hamersley Basin of subtropical northwest Australia. J. Hydrol. 475, 281–293.

Egozcue, J.J., Pawlowsky-Glahn, V., 2005. Groups of parts and their balances in compositional data analysis. Math. Geol. 37, 795–828.

Egozcue, J.J., Pawlowsky-Glahn, V., Mateu-Figueras, G., Barcelo-Vidal, C., 2003. Isometric logratio transformations for compositional data analysis. Math. Geol. 35, 279–300.

Engle, M.A., Blondes, M.S., 2014. Linking compositional data analysis with thermodynamic geochemical modeling: oilfield brines from the Permian Basin, USA. J. Geochem. Explor. 141, 61–70.

Engle, M.A., Rowan, E.L., 2014. Geochemical evolution of produced waters from hydraulic fracturing of the Marcellus Shale, northern Appalachian Basin: a multivariate compositional data analysis approach. Int. J. Coal Geol. 126, 45–56.

Epstein, S., Mayeda, T., 1953. Variation of O^{18} content of waters from natural sources. Geochim. Cosmochim. Acta 4, 213–224.

Filzmoser, P., Hron, K., Reimann, C., 2009. Principal component analysis for compositional data with outliers. Environmetrics 20, 621–632.

Filzmoser, P., Hron, K., Reimann, C., 2010. The bivariate statistical analysis of environmental (compositional) data. Sci. Total Environ. 408, 4230–4238.

Foppen, J.W.A., 2002. Impact of high-strength wastewater infiltration on groundwater quality and drinking water supply: the case of Sana'a, Yemen. J. Hydrol. 263, 198–216.

Foster, S.S.D., 2001. The interdependence of groundwater and urbanisation in rapidly developing cities. Urban Water 3, 185–192.

Fukada, T., Hiscock, K.M., Dennis, P.F., Grischek, T., 2003. A dual isotope approach to identify denitrification in groundwater at a river-bank infiltration site. Water Res. 37, 3070–3078.

Gantumur, B., Wu, F., Zhao, Y., Vandansambuu, B., Dalaibaatar, E., Itirittiphan, F., Shaimurat, D., 2017. Implication of relationship between natural impacts and land use/land cover (LULC) changes of urban area in Mongolia. Proceedings of SPIE 10431, Remote Sensing Technologies and Applications in Urban Environments II, 104310M (4 October 2017) https://doi.org/10.1117/12.2278360.

Garmaev, E.Z., Bolgov, M.V., Ayurzhanaev, A.A., Tsydypov, B.Z., 2019. Water resources in Mongolia and their current state. Russ. Meteorol. Hydrol. 44, 659–666. https://doi.org/10.3103/S1068373919100030.

Gat, J.R., 1996. Oxygen and hydrogen isotopes in the hydrologic cycle. Annu. Rev. Earth Planet. Sci. 24, 225–262.

Gehre, M., Hoefling, R., Kowski, P., Strauch, G., 1996. Sample preparation device for quantitative hydrogen isotope analysis using chromium metal. Anal. Chem. 68, 4414–4417.

Gonfiantini, R., Roche, M.A., Olivry, J.C., Fontes, J.C., Zuppi, G.M., 2001. The altitude effect on the isotopic composition of tropical rains. Chem. Geol. 181, 147–167.

Hofmann, J., Watson, V., Scharaw, B., 2014. Groundwater quality under stress: contaminants in the Kharaa River basin (Mongolia). Environ. Earth Sci. 73, 629–648.

Hosono, T., Wang, C.H., Umezawa, Y., Nakano, T., Onodera, S.I., Nagata, T., Yoshimizu, C., Tayasu, I., Taniguchi, M., 2011. Multiple isotope (H, O, N, S and Sr) approach elucidates complex pollution causes in the shallow groundwaters of the Taipei urban area. J. Hydrol. 397, 23–36.

Itoh, M., Takemon, Y., Makabe, A., Yoshimizu, C., Kohzu, A., Ohte, N., Tumurskh, D., Tayasu, I., Yoshida, N., Nagata, T., 2011. Evaluation of wastewater nitrogen transformation in a natural wetland (Ulaanbaatar, Mongolia) using dual-isotope analysis of nitrate. Sci. Total Environ. 409, 1530–1538.

Jurado, A., Vàzquez-Suñé, E., Soler, A., Tubau, I., Carrera, J., Pujades, E., Anson, I., 2013. Application of multi-isotope data (O, D, C and S) to quantify redox processes in urban groundwater. Appl. Geochem. 34, 114–125.

Kamata, T., Reichert, J., Tsevegmid, T., Kim, Y., Sedgewick, B., 2010. Managing Urban Expansion in Mongolia: Best Practices in Scenario-based Urban Planning. The World Bank, Washington, D.C https://doi.org/10.1596/978-0-8213-8314-8.

Karthe, D., Heldt, S., Houdret, A., Borchardt, D., 2014. IWRM in a country under rapid transition: lessons learnt from the Kharaa River Basin, Mongolia. Environ. Earth Sci. 73, 681–695.

Kendall, C., Aravena, R., 2000. Nitrate isotopes in groundwater systems. Environmental Tracers in Subsurface Hydrology. Springer.

Khishigjargal, M., Dulamsuren, C., Leuschner, H.H., Leuschner, C., Hauck, M., 2014. Climate effects on inter-and intra-annual larch stemwood anomalies in the Mongolian forest-steppe. Acta Oecol. 55, 113–121.

Khosravi, K., Sartaj, M., Tsai, F.T., Singh, V.P., Kazakis, N., Melesse, A.M., Prakash, I., Tien Bui, D., Pham, B.T., 2018. A comparison study of DRASTIC methods with various objective methods for groundwater vulnerability assessment. Sci. Total Environ. 642, 1032–1049.

Kim, H.R., Yu, S., Oh, J., Kim, K.H., Lee, J.H., Moniruzzaman, M., Kim, H.K., Yun, S.T., 2019. Nitrate contamination and subsequent hydrogeochemical processes of shallow groundwater in agro-livestock farming districts in South Korea. Agric. Ecosyst. Environ. 273, 50–61.

Kong, F., Song, J., Zhang, Y., Fu, G., Cheng, D., Zhang, G., Xue, Y., 2019. Surface water-groundwater interaction in the Guanzhong section of the Weihe River Basin, China. Groundwater 57 (4), 647–660.

Kurihara, T., Tsukada, K., Otoh, S., Kashiwagi, K., Chuluun, M., Byambadash, D., Boijir, B., Gonchigdorj, S., Nuramkhan, M., Niwa, M., Tokiwa, T., 2009. Upper Silurian and Devonian pelagic deep-water radiolarian chert from the Khangai–Khentei belt of Central Mongolia: evidence for Middle Paleozoic subduction-accretion activity in the Central Asian Orogenic Belt. J. Asian Earth Sci. 34, 209–225.

Lee, K.J., Yun, S.T., Yu, S., Kim, K.H., Lee, J.H., Lee, S.H., 2019. The combined use of self-organizing map technique and fuzzy c-means clustering to evaluate urban groundwater quality in Seoul metropolitan city, South Korea. J. Hydrol. 569, 685–697.

Lu, Q., Sato, M., 2007. Quantitative Hydrogeological Study of an Unconfined Aquifer by GPR along Tuul River in Ulaanbaatar. Report of Center for Northeast Asian Studies. Tohoku University https://doi.org/10.15068/00147208.

Mengis, M., Schif, S.L., Harris, M., English, M.C., Aravena, R., Elgood, R.J., MacLean, A., 1999. Multiple geochemical and isotopic approaches for assessing ground water NO_3^- elimination in a riparian zone. Ground Water 37, 448–457.

Ming, X., Groves, C., Wu, X., Chang, L., Zheng, Y., Yang, P., 2020. Nitrate migration and transformations in groundwater quantified by dual nitrate isotopes and hydrochemistry in a karst World Heritage site. Sci. Total Environ. 735, 138907.

Morán-Ramírez, J., Ledesma-Ruiz, R., Mahlknecht, J., Ramos-Leal, J.A., 2016. Rock-water interactions and pollution processes in the volcanic aquifer system of Guadalajara, Mexico, using inverse geochemical modeling. Appl. Geochem. 68, 79–94.

Munkhsuld, E., Ochir, A., Koop, S., Leeuwen, K.V., Batbold, T., 2020. Application of the city blueprint approach in landlocked Asian countries: a case study of Ulaanbaatar, Mongolia. Water 12, 199. https://doi.org/10.3390/w12010199.

Nriagu, J., Nam, D.H., Ayanwola, T.A., Dinh, H., Erdenechimeg, E., Ochir, C., Bolormaa, T.A., 2012. High levels of uranium in groundwater of Ulaanbaatar, Mongolia. Sci. Total Environ. 414, 722–726.

Oiro, S., Comte, J.-C., Soulsby, C., Walraevens, K., 2018. Using stable water isotopes to identify spatio-temporal controls on groundwater recharge in two contrasting East African aquifer systems. Hydrol. Sci. J. 63, 862–877.

Parkhurst, D.L., Appelo, C.A.J., 1999. User's Guide to Phreeqc (version 2) – A Computer Program for Speciation, Batch-reaction, One Dimensional Transport and Inverse Geochemical Calculation. USGS Water-Resources Investigation Report 99-4259. U.S. Geological Survey, Denver (312p).

Purevjav, N., Roser, B., 2013. Geochemistry of Silurian–carboniferous sedimentary rocks of the Ulaanbaatar terrane, Hangay–Hentey belt, central Mongolia: provenance, paleoweathering, tectonic setting, and relationship with the neighbouring Tsetserleg terrane. Chem. Erde-Geochem. 73, 481–493.

Sato, T., Kimura, F., Kitoh, A., 2007. Projection of global warming onto regional precipitation over Mongolia using a regional climate model. J. Hydrol. 333, 144–154.

SDOU, 2015. Statistics Department of Ulaanbaatar. The SDOU Database. Accessible at:. http://ubstat.mn/Statistics.

Semadeni-Davies, A., Hernebring, C., Svensson, G., Gustafsson, L.G., 2008. The impacts of climate change and urbanisation on drainage in Helsingborg, Sweden: combined sewer system. J. Hydrol. 350, 100–113.

Shi, P., Zhang, Y., Song, J., Lia, P., Wang, Y., Zhang, X., Lia, Z., Bi, Z., Zhang, X., Qin, Y., Zhu, T., 2019. Response of nitrogen pollution in surface water to land use and social-economic factors in the Weihe River watershed, northwest China. Sust. Cities Soc. 50, 101658.

Silva, S.R., Kendall, C., Wilkison, D.H., Ziegler, A.C., Chang, C.C., Avanzino, R.J., 2000. A new method for collection of nitrate from fresh water and the analysis of nitrogen and oxygen isotope ratios. J. Hydrol. 228, 22–36.

Takeuchi, M., Tsukada, K., Suzuki, T., Nakane, Y., et al., 2012. Stratigraphy and geological structure of the Paleozoic system around Ulaanbaatar, Mongolia. Bull. Nagoya Univ. Museum 28, 1–18.

Templ, M., Hron, K., Filzmoser, P., 2011. robCompositions: Robust Estimation for Compositional Data. Manual and Package, Version 1(4).

Tsujimura, M., Abe, Y., Tanaka, T., Shimada, J., Higuchi, S., Yamanaka, T., Davaa, G., Oyunbaatar, D., 2007a. Stable isotopic and geochemical characteristics of groundwater in Kherlen River basin, a semi-arid region in eastern Mongolia. J. Hydrol. 333, 47–57.

Tsujimura, M., Sasaki, L., Yamanaka, T., Sugimoto, A., Li, S.G., Matsushima, D., Kotani, A., Saandar, M., 2007b. Vertical distribution of stable isotopic composition in atmospheric water vapor and subsurface water in grassland and forest sites, eastern Mongolia. J. Hydrol. 333, 35–46.

Tsutsumida, N., Saizen, I., Matsuoka, M., Ishii, R., 2015. Addressing urban expansion using feature-oriented spatial data in a peripheral area of Ulaanbaatar, Mongolia. Habitat Int. 47, 196–204.

UNDP (United Nations Development Programme), 2008. Water and Sanitation in Mongolia 2008–2011. UNDP Report, Ulaanbaatar, Mongolia. https://www.undp.org/content/dam/undp/documents/projects/MNG/00049774_UNDP%20Project_Water%20and%20sanitation.pdf.

UN-HABITAT (United Nations Human Settlements Programme), 2010. Citywide Pro-Poor Ger Area Upgrading Strategy of Ulaanbaatar City. UN-HABITAT Mongolia Office https://unhabitat.org/sites/default/files/documents/2019-05/gusip_output_1.6_-_citywide_pro-poor_ger-area_upgrading_strategy_november2010.pdf.

United Nations, 2003. The ground beneath our feet: a factor in urban planning. Atlas of Urban Geology. vol. 14. United Nations Publication.

United Nations, 2019. World Urbanization Prospects The 2018 Revision. United Nations, Department of Economic and Social Affairs https://population.un.org/wup/Publications/Files/WUP2018-Report.pdf.

Vairavamoorthy, K., Mansoor, M.A.M., 2006. Demand management in developing countries. In: Butler, D., Memon, F.A. (Eds.), Water Demand Management. IWA Publishing, London, UK, pp. 180–214.

Warburton, D., Warburton, N., Wigfall, C., Chimedsuren, O., Lodoisamba, D., Lodoysamba, S., Jargalsaikhan, B., 2018. Impact of seasonal winter air pollution on health across the lifespan in Mongolia and some putative solutions. AnnalsATS 15 (Suppl. 2), S86–S90. https://doi.org/10.1513/AnnalsATS.201710-758MG.

WHO, 2008. Guidelines for Drinking-Water Quality. https://www.who.int/water_sanitation_health/dwq/fulltext.pdf.

WHO/UNICEF (World Health Organization and United Nations Children"s Fund), 2008. Progress on Drinking Water and Sanitation: Special Focus on Sanitation. Report of WHO/UNICEF Joint Monitoring Programme for Water Supply and Sanitation (JMP) (ISBN 978 92 806 4313 8).

Xue, D., Botte, J., De Baets, B., Accoe, F., Nestler, A., Taylor, P., Van Cleemput, O., Berglund, M., Boeckx, P., 2009. Present limitations and future prospects of stable isotope methods for nitrate source identification in surface- and groundwater. Water Res. 43, 1159–1170.

Yamanaka, T., Tsujimura, M., Oyunbaatar, D., Davaa, G., 2007. Isotopic variation of precipitation over eastern Mongolia and its implication for the atmospheric water cycle. J. Hydrol. 333, 21–34.